Intrinsic ripples in graphene

A. Fasolino, J. H. Los and M. I. Katsnelson

Institute for Molecules and Materials,

Radboud University Nijmegen, 6525 ED Nijmegen, The Netherlands

(Dated: February 1, 2008)

The stability of two-dimensional (2D) layers and membranes is subject of a long standing theoretical debate. According to the so called Mermin-Wagner theorem [1], long wavelength fluctuations destroy the long-range order for 2D crystals. Similarly, 2D membranes embedded in a 3D space have a tendency to be crumpled [2]. These dangerous fluctuations can, however, be suppressed by anharmonic coupling between bending and stretching modes making that a two-dimensional membrane can exist but should present strong height fluctuations [2, 3, 4]. The discovery of graphene, the first truly 2D crystal [5, 6] and the recent experimental observation of ripples in freely hanging graphene [7] makes these issues especially important. Beside the academic interest, understanding the mechanisms of stability of graphene is crucial for understanding electronic transport in this material that is attracting so much interest for its unusual Dirac spectrum and electronic properties [8, 9, 10, 11]. Here we address the nature of these height fluctuations by means of straightforward atomistic Monte Carlo simulations based on a very accurate many-body interatomic potential for carbon [12]. We find that ripples spontaneously appear due to thermal fluctuations with a size distribution peaked around 70Å which is compatible with experimental findings [7] (50-100 Å) but not with the current understanding of stability of flexible membranes [2, 3, 4]. This unexpected result seems to be due to the multiplicity of chemical bonding in carbon.

The phenomenological theories for flexible membranes [2, 3, 4] are derived in the continuum limit without including any microscopic feature and their applicability to graphene in the interesting range of temperatures, sample sizes etc. is not evident. We present Monte Carlo simulations of the equilibrium structure of single layer graphene. By monitoring the normal-normal correlation functions we can directly compare our results to the predictions of the existing theories. The effect of interest is crucially dependent on acoustical phonons and interactions between them and therefore the simulations require samples much larger than interatomic distances, typically many thousands of atoms at thermal equilibrium, making prohibitive ab-initio simulations a la Car-Parrinello [13]. However, for carbon a very accurate description of energetic and thermodynamic properties of different phases is provided by the effective many body potential LCBOPII [12, 14]. This bond order potential is constructed in such a way as to provide a unified description of the energetics and elastic constants of all

carbon phases as well as the energy characteristics of different defects with accuracy comparable to experimental accuracy. We find clear deviations from harmonic behavior for long wavelength fluctuations but, instead of the expected power-law scaling at long wavelengths, we find a marked maximum of fluctuations with wavelength of about 70 Å. Against the expectations, we also find a stiffening of the bending rigidity with increasing temperature. We relate these features to fluctuations in bond length that in carbon signal a partial change from conjugated to single/double bonds, with consequent deviations from planarity.

We perform atomistic Monte Carlo (MC) simulations based on the standard Metropolis algorithm for approximately squared samples of different sizes (see Table I) with periodic boundary conditions. We always start with completely flat graphene layers to avoid any bias. Typically we used 400000 MC steps (1 MC step corresponds to N attempts to a coordinate change) to equilibrate and half a million for averaging. Every 5 MC steps, we allow for isotropic size fluctuations. The energy of a given configuration is evaluated according to the bond order potential LCBOPII developed in the recent past [12]. This potential is based on a large database of experimental and theoretical data for molecules and solids and has been proven to describe very well thermodynamic and structural properties of all phases of carbon and its phase diagram in a wide range of temperatures and pressures [12, 14]. We believe that LCBOPII can give a good description of graphene because it reproduces correctly the elastic properties of graphene and yields structure and energetics of vacancies in graphene in good agreement with *ab initio* calculations [15]. Of particular importance here, is that bond order potentials correlate coordination, bond length and bond strength, allowing changes between single, double and conjugated bonds with the correct energetics. Most simulations have been performed at room temperature $T = 300$ K but we have also simulated some of the structures at very high temperature $T = 3500$ K close to the bulk graphite melting to study qualitatively temperature effects.

A typical snapshot of graphene at room temperature is shown in Fig.1. The first thing to notice is that height fluctuations are present at equilibrium. We find a very broad distribution of height displacements $\overline{h}$ with a typical size of order of 0.6 Å for the $N = 8640$ sample, comparable to the interatomic distance 1.42 Å.

The natural way to analyse further our results is to compare them to the results and predictions of the phenomenological theories of thermal fluctuations in flexible membranes [2, 3, 4]. To this purpose it is worth to review in some detail the main ideas and results of

these theories [2, 3, 4] that are not of common knowledge outside the soft condensed matter community. The primary quantities are the two-component displacement vector in the plane $\mathbf{u}$, the out of plane displacement out of plane h and the normal unit vector $\mathbf{n}$ with in-plane component $-\nabla h/\sqrt{1+(\nabla h)^2}$ illustrated in Fig.2. The elastic energy of the membrane is given by

$$E = \int d^2x \left[\frac{\kappa}{2} \left(\nabla^2 h \right)^2 + \mu \overline{u}_{\alpha\beta}^2 + \frac{\lambda}{2} \overline{u}_{\alpha\alpha}^2 \right] \tag{1}$$

where κ is the bending rigidity, μ and λ are Lamé parameters and $\overline{u}_{\alpha\beta}$ is the deformation tensor:

$$\overline{u}_{\alpha\beta} = \frac{1}{2} \left(\frac{\partial u_\alpha}{\partial x_\beta} + \frac{\partial u_\beta}{\partial x_\alpha} + \frac{\partial h}{\partial x_\alpha} \frac{\partial h}{\partial x_\beta} \right). \tag{2}$$

In harmonic approximation, by neglecting the last, non linear, term in the deformation tensor (2), the bending (h) and stretching ($\mathbf{u}$) modes are decoupled. In this approximation the Fourier components of the bending correlation function with wavevector $\mathbf{q}$ is

$$\left\langle |h_{\mathbf{q}}|^2 \right\rangle = \frac{TN}{\kappa S_0 q^4} \tag{3}$$

where N is the number of atoms, $S_0 = L_x L_y / N$ is the area per atom and T is the temperature in units of energy. In this approximation, the mean square displacement in the direction normal to the layer is

$$\left\langle h^2 \right\rangle = \sum_{\mathbf{q}} \left\langle |h_{\mathbf{q}}|^2 \right\rangle \propto \frac{T}{\kappa} L^2 \tag{4}$$

where L is a typical linear sample size. The correlation function of the normals

$$G(q) = \left\langle |\mathbf{n}_{\mathbf{q}}|^2 \right\rangle = q^2 \left\langle |h_{\mathbf{q}}|^2 \right\rangle \tag{5}$$

in this approximation becomes

$$G_0(q) = \frac{TN}{\kappa S_0 q^2} \tag{6}$$

which implies that the mean square angle between the normals is logarithmically divergent as $L \to \infty$ [2]. This behaviour indicates the tendency to crumpling of membranes due to thermal fluctuations.

Deviations from this harmonic behaviour, namely anharmonic coupling between bending and stretching modes, can stabilize the flat phase by suppressing the long wavelength fluctuations [2, 3, 4]. In this case the corresponding correlation function of the normals is given by the Dyson equation

$$G_a^{-1}(q) = G_0^{-1}(q) + \Sigma(q) \tag{7}$$

with self energy

$$\Sigma(q) = \frac{AS_0}{Nq^2}\left(\frac{q}{q_0}\right)^{\eta} \tag{8}$$

where $q_0 = 2\pi\sqrt{B/\kappa}$, B being the two-dimensional bulk modulus, η is the anomalous rigidity exponent and A is a numerical factor.

The simplest way to derive this expression is to use the self-consistent perturbation theory [4] which gives $\eta \approx 0.8$ in reasonable agreement with the results of Monte Carlo simulation for a model of tethered membranes [16]. However, Eqs.(7),(8) can be written from a more general scaling consideration [3], q_0 being the only factor with dimension of an inverse length that can be constructed from relevant parameters of this theory. As a result of this anharmonic coupling, the typical height of fluctuations in the direction normal to the membrane is much smaller than the one given by Eq.(4) and scales with the sample size as L^{ζ}, with $\zeta = 1 - \eta/2$. Nevertheless, the fluctuations are still anomalously large and they can be much larger than the interatomic distance for large samples. Thus, the theory predicts an intrinsic tendency to ripple formation. At the same time, the amplitude $\overline{h} \propto L^{\zeta}$ of these transverse fluctuations remains much smaller than the sample size and preserves the long-range order of the normals so that the membrane can be considered as approximately flat and not crumpled.

Another structural issue is the existence of long range crystallographic order in membranes that can be destroyed by a finite concentration of topological defects, namely dislocations and disclinations. For the case of 2D crystals in 2D space both types of defects have infinite energy as $L \to \infty$: the elastic energy of dislocations grows as $\ln(L)$, and of disclinations as L. A general analysis [2] (Chap. 6) for flexible membranes shows that these divergencies are suppressed by bending in such a way that the energy of disclinations behaves as $\ln(L)$ whereas that of dislocations remains finite, and of the order of κ. This means that the orientational order survives whereas translational order is destroyed by spontaneous creation of dislocations. However, the corresponding correlation length is $\propto \exp(const \cdot \kappa/T)$ which makes this mechanism completely irrelevant for covalently bonded layers such as graphene, with $\kappa \approx 1.17$ eV [17]. Indeed, we never observe any topological defect in our simulations also at very high temperature, nor any experimental evidence of their existence has been reported [7].

To obtain a quantitative comparison with these theoretical predictions for the spatial

distribution of the ripples, we have calculated numerically the Fourier components of the correlation function of the normals $G(q)$ for q_x and q_y multiples of $2\pi/L_x$ and $2\pi/L_y$ respectively. To our surprise, our numerical results are not described by this general theory.

In Fig.3 we show $G(q)$ at $T = 300$ K for all considered samples and in Fig.4 we compare the results at two temperatures for the sample $N = 8640$. First of all, there is a whole range of wave vectors where the harmonic approximation given by Eq.(6) is quite accurate. The interval is restricted above close to the Bragg peaks and in the limit of small q. The deviations are opposite at the two sides. The rigidity $\kappa = 1.1$ eV extracted from the data at $T = 300$ K by comparison with Eq.(6) is in very good agreement with the experimental value of 1.2 eV derived from the phonon spectrum of graphite [17]. Surprisingly, the same comparison at $T = 3500$ K gives a higher value $\kappa \approx 2.0$ eV whereas the contimuum theory [2] predicts the opposite trend $\kappa(T) \approx \kappa - (3T/4\pi)\ln(L/a)$. This is due to the peculiar character of bonding in carbon. In the ground state of graphene all bonds are equivalent. However, even at room temperature, there is a large probability of having an asymmetric distribution of short/long (strong/weak) bonds, associated with local deviations from planarity. Indeed, the radial distribution functions shown in Fig.5 for both temperatures show a broad distribution of first neighbors bond lengths, going down to the length of double bonds in carbon of 1.31 Å at high temperature. Changes of bond conjugation are also the reason for the negative thermal expansion coefficient in graphene found in ab-initio calculations [18]. We observe a 0.13 % contraction of the lattice spacing at $T = 300$ K, in good agrement with the 0.11 % of Ref. 18. We believe that it is the ability of carbon to form different types of bonding that makes graphene different from a generic two-dimensional crystal.

At small q, the behaviour of $G(q)$ is not described by the harmonic approximation $G_0(q)$ nor by the anharmonic expression $G_a(q)$. The most remarkable feature of $G(q)$ is a maximum instead of the power law dependence $G_a(q)$ that implies the absence of any relevant length scale in the system. The presence of this maximum, instead, means that there is a preferred average value of about 70 Å. This length is also recognizable in real space images, as shown by the arrows in Fig.1. Indeed, the two samples that are smaller than this length do not show this decrease of $G(q)$ at low q. The results at $T = 3500$ K confirm this picture but with the maximum shifted to a larger q corresponding to a length of roughly 30 Å. This temperature dependence of the typical ripple lengthscale should be measurable.

The preferable length that we find is reminiscent of the "avoided criticality" scenario in

frustrated systems near second-order phase transitions [19]. Such systems have an intrinsic tendency to be modulated and to form some inhomogeneous patterns that destroys the scaling. It is known that some soft condensed matter membranes tend to spontaneous bending and ripple formation [20, 21, 22] but this behaviour for elemental solids like graphene is rather unexpected.

The results obtained are relevant not only for a better understanding of the stability and structure of graphene but also of electronic transport. The fluctuations of normals leads to a modulation of the hopping integrals and are bound to affect the electronic structure [23, 24]. Knowledge of the normal-normal correlation functions is necessary for the calculation of the electron scattering by ripples.

The cleavage technique that has led to the discovery of graphene has already been applied to other layered materials, like BN [5], so that the investigation of structural properties of one atom thick layers is important for a whole new class of systems. We have found that even fluctuations at the scale of tens of interatomic distances cannot be described by continuum medium theory. It will be very instructive to carry out systematic experimental and theoretical investigations of other two-dimensional crystals to understand which properties are common to flexible membranes and which ones are consequences of particular features of the chemical bonding and interatomic interactions.

Acknowledgements. We are thankful to Jan Kees Maan for suggestions and critical reading of the manuscript, Andre Geim, Kostya Novoselov and Jannik Meyer for helpful discussions. This work was supported by the Stichting Fundamenteel Onderzoek der Materie (FOM) with financial support from the Nederlandse Organisatie voor Wetenschappelijk Onderzoek (NW

---

[1] Mermin, N. D. Crystalline order in two dimensions. *Phys. Rev.* **176**, 250-254 (1968).

[2] Nelson, D. R., Piran, T. & Weinberg, S. (Editors), *Statistical Mechanics of Membranes and Surfaces*, World Scientific, Singapore (2004).

[3] Nelson, D. R. & Peliti, L. Fluctuations in membranes with crystalline and hexatic order. *J. Physique* **48**, 1085-1092 (1987).

[4] Radzihovsky, L. & Le Doussal, P. Self-consistent theory of polymerized membranes. *Phys.*

Rev. Lett. **69**, 1209-1212 (1992).

[5] Novoselov, K. S. et al. Two-dimensional atomic crystals. *Proc. Natl Acad. Sci. USA* **102**, 10451-10453 (2005).

[6] Novoselov, K. S. et al. Electric field effect in atomically thin carbon films. *Science* **306**, 666-669 (2004).

[7] Meyer, J. C. et. al. The structure of suspended graphene membrane. *Nature* **446**, 60-63 (2007).

[8] Novoselov, K. S. et al. Two-dimensional gas of massless Dirac fermions in graphene. *Nature* **438**, 197-200 (2005).

[9] Zhang, Y., Tan, J. W., Stormer, H. L. & Kim, P. Experimental observation of the quantum Hall effect and Berry's phase in graphene. *Nature* **438**, 201-204 (2005).

[10] Geim, A. K. & Novoselov, K. S. The rise of graphene. *Nature Mater.* **6**, 183-191 (2007).

[11] Katsnelson, M. I. Graphene: Carbon in two dimensions. *Mater. Today* **10**, Issue 1&2, 20-27 (2007).

[12] Los, J. H., Ghiringhelli, L. M., Meijer, E. J. & Fasolino, A. Improved long-range reactive bond-order potential for carbon. I. Construction. *Phys. Rev. B* **72**, 214102 (2005).

[13] Car, R. & Parrinello, M. Unified approach for molecular dynamics and density-functional theory. *Phys. Rev. Lett.* **55**, 2471-2474 (1985).

[14] Ghiringhelli, L. M., Los, J. H., Meijer, E. J., Fasolino, A. & Frenkel D. Modeling the Phase Diagram of Carbon. *Phys. Rev. Lett.* **94**, 145701 (2005).

[15] Carlsson, J. M. & Scheffler M. Structural, Electronic, and Chemical Properties of Nanoporous Carbon. *Phys. Rev. Lett.* **96**, 046806 (2006)

[16] Bowick, M. J. Fixed-connectivity membranes, chapter 11 in Ref. 2.

[17] Niclow, R., Wakabayashi, N. & Smith, H.G. Lattice dynamics of pyrolytic graphite. *Phys. Rev. B* **5**, 4951 - 4962 (1972).

[18] Mounet, N. & Marzari, N. First-principles determination of the structural, vibrational and thermodynamic properties of diamond, graphite, and derivatives. *Phys. Rev. B* **71**, 205214 (2005).

[19] Tarjus, G., Kivelson, S. A., Nussinov, Z. & Viot, P. The frustrated-based approach of supercooled liquids and the glass transition: A review and critical assessment. *J. Phys.: Condens. Matter* **17**, R1143-R1182 (2005).

[20] Katsnelson, M. I. & Fasolino, A. Solvent-driven formation of bolaamphiphilic vesicles. *J. Phys.*

Chem. B **110**, 30-32 (2006).

[21] Manyuhina, O. V. et al. Anharmonic magnetic deformation of self-assembled molecular nanocapsules. *Phys. Rev. Lett.* **98**, 146101 (2007).

[22] Lubensky, T. C. & MacKintosh, F. C. Theory of "rippled" phases of liquid bilayers. *Phys. Rev. Lett.* **71**, 1565-1568 (1993).

[23] Morozov, S. V. et. al. Strong suppression of weak localization in graphene. *Phys. Rev. Lett.* **97**, 016801 (2006).

[24] Castro Neto, A. H. & Kim, E. A. Charge inhomogeneity and the structure of graphene sheets. *E-print at arxiv.org: cond-mat/0702562.*

N	p	q	L_x(Å)	L_y(Å)
240	10	6	24.59	25.56
960	20	12	49.29	51.12
2160	30	18	73.78	76.68
4860	45	27	110.68	115.02
8640	60	36	147.57	153.36
19940	90	54	221.36	230.04

TABLE I: Details of the simulated samples. The initial, roughly squared, box is defined by $(L_x, L_y) = (2p|\mathbf{a}_1|, q|\mathbf{a}_1 + 2\mathbf{a}_2|)$ where $\mathbf{a}_1$ and $\mathbf{a}_2$ are the in-plane lattice vectors $\mathbf{a}_1 = a\sqrt{3}\mathbf{x}$, $\mathbf{a}_2 = a\sqrt{3}/2\mathbf{x}+3/2\mathbf{y}$, $\mathbf{x}$ and $\mathbf{y}$ being cartesian unit vectors.

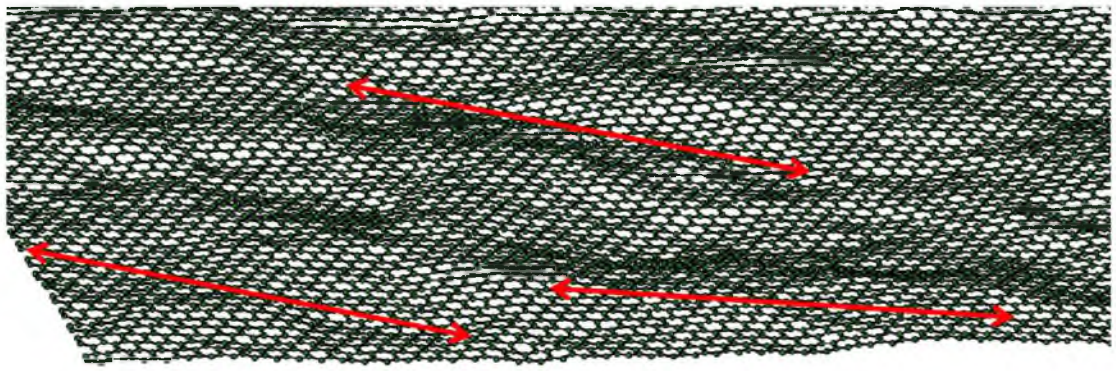

FIG. 1: Snapshot of the $N = 8640$ sample at $T = 300$ K. The red arrows are 70 Å long.

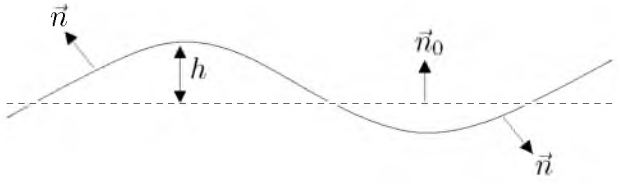

FIG. 2: Sketch of a flexible membrane (solid line). h is the out of plane deviation with respect to the $z = 0$-plane (dashed line) defined by the center of mass. The unit vector $\vec{n}$ and $\vec{n}_0$ are the normals to each point in the membrane and in the reference plane respectively.

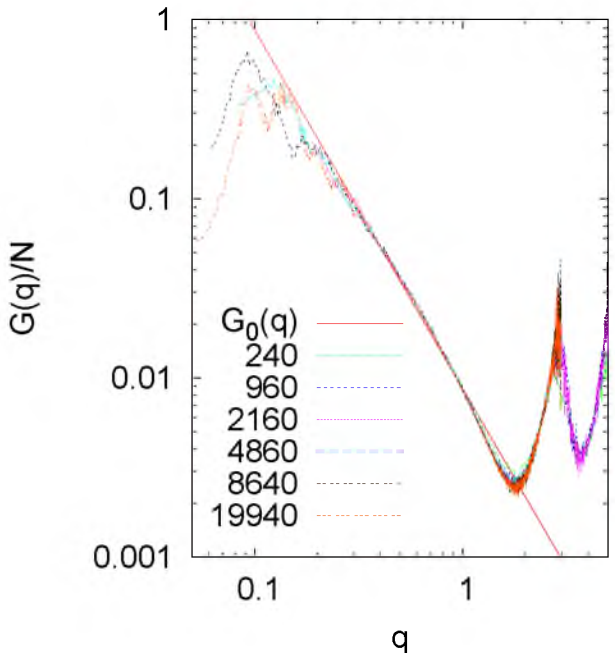

FIG. 3: Normal-normal correlation function $G(q)/N$ for all studied samples. The solid straight line gives the harmonic power law behaviour $G_0(q)/N$ with κ=1.1 eV. Deviations from harmonic behavior occur for q close to the Bragg peaks at $q = 4\pi/3a = 2.94$ Å^{-1} and $q = 4\pi/\sqrt{(3)}a = 5.11$ Å^{-1} with $a = 1.42$ Å and at small q where the peak of $G(q)$ at $q \approx 0.1$ signals a preferred length scale of about 70 Å.

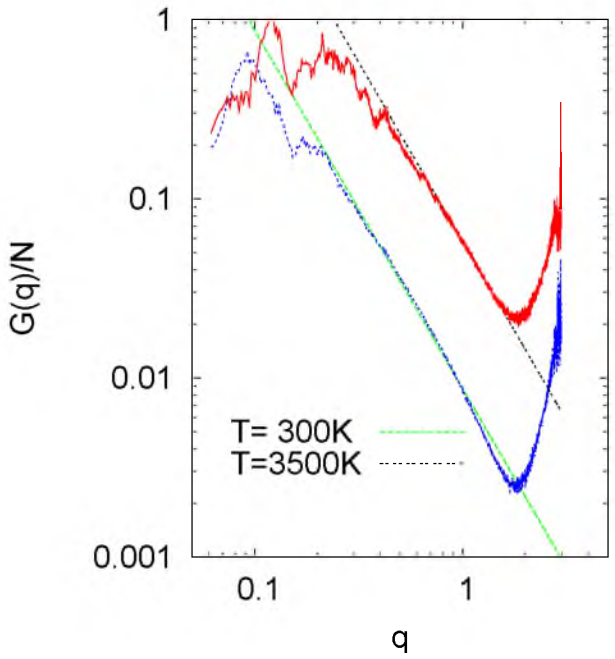

FIG. 4: Normal-normal correlation function $G(q)/N$ for the $N = 8640$ sample at $T = 300$ K and $T = 3500$ K. The solid straight line gives the harmonic power law behaviour $G_0(q)$ with κ=1.1 eV at $T = 300$ and κ=2.0 eV at $T = 3500$ K.

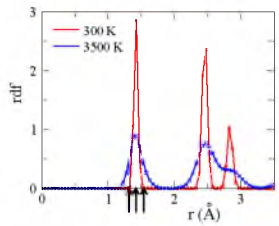

FIG. 5: Radial distribution function for the $N = 8640$ sample at $T = 300$ K and $T = 3500$ K as a function of interatomic distances in Å. The arrows indicate the length of double ($r = 1.31$ Å), conjugated ($r = 1.42$ Å) and single ($r = 1.54$ Å) bonds.

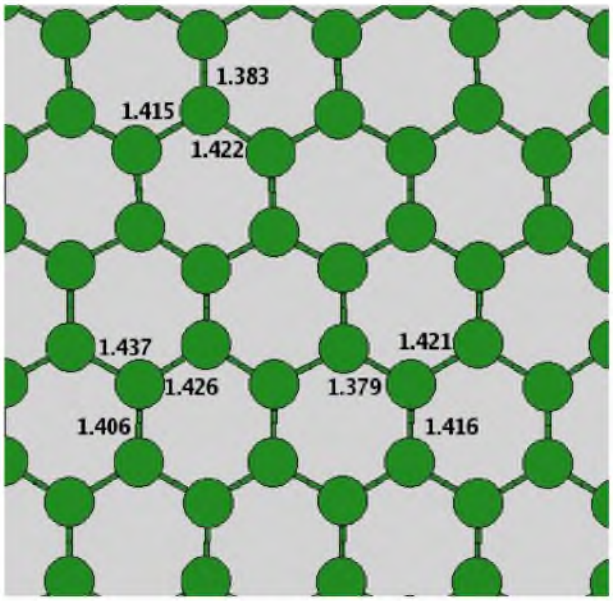

FIG. 6: Portion of one typical configuration of the $N = 8640$ sample at $T = 300$ K. The numbers indicate the bond length in Å. Notice that often one of the bonds with first neighbours is much shorter than the other two.